

Fano-Kondo and the Kondo-box regimes crossover in a quantum dot coupled to a quantum box

Victor .M. Apel,¹ Pedro A. Orellana,² Monica Pacheco,² and Enrique V. Anda³

¹*Departamento de Física, Universidad Católica del Norte, Casilla 1280, Antofagasta, Chile*

²*Departamento de Física, Universidad Técnica F. Santa María, Casilla Postal 110 V, Valparaíso, Chile*

³*Departamento de Física, P. U. Católica do Rio de Janeiro, C.P. 38071-970, Rio de Janeiro, R.J, Brazil*

In this work, we study the Kondo effect of a quantum dot (QD) connected to leads and to a discrete set of one particle states provided by a quantum box represented by a quantum ring (QR) pierced by a magnetic flux side attached to the QD. The interplay between the bulk Kondo effect and the so called Kondo box regime is studied. In this system the QR energies can be continuously modified by the application of the magnetic field. The crossover between these two regimes is analyzed by changing the connection of the QD to the QR from the weak to the strong coupling regime. In the weak coupling regime, the differential conductance develops a sequence of Fano-Kondo antiresonances due to destructive interferences between the discrete quantum ring levels and the conducting Kondo channel provided by the leads. In the strong coupling regime the differential conductance has very sharp resonances when one of the Kondo discrete sub-level characterizing the Kondo box is tuned by the applied potential. The conductance, the current fluctuations and the Fano coefficient result to be the relevant physical magnitudes to be analyzed to reveal the physical properties of these two Kondo regimes and the crossover region between them. The results were obtained by using the Slave Boson Mean Field Theory (SBMFT).

I. INTRODUCTION

Electronic transport through nanoscopic systems, as quantum dots (QDs) has been extensively studied in the last decade¹⁻⁴. The QDs allow the systematic study of quantum-coherent effects as Kondo, Fano and Aharonov-Bohm effects due to the possibility of continuous tuning the relevant parameters governing the properties of these regimes, in equilibrium and nonequilibrium situations^{1,4-8}.

Kondo effect in QDs dominates the electronic transport properties due to the strong many-body correlations between the conduction band electron spins in the leads and the localized spin in the QD, when the temperature T is below the Kondo temperature T_k ^{2,9}. The main signature of the Kondo state in nanosystems as a QD connected to two leads is the enhancement of the conductance below T_k up to the unitary limit $(2e^2/h)^2$. In this configuration electrons transmitted from one electrode to the other necessarily pass through the QD. It is presently known that coupled quantum dots exhibit the electronic counterpart of the Fano and Dicke effects and that they can be controlled by the magnetic flux and quantum-dot asymmetry¹⁰⁻¹³. The emergence of Fano resonances requires two scattering channels: a discrete level and a broad continuum band⁵. Present understanding of electron transport properties of quantum dots is based mainly on direct current measurements. However, additional information can be obtained from fluctuations of the current¹⁴⁻²². Electronic current through any conductor fluctuates with time reflecting charge granularity. This phenomenon is referred in the literature as shot noise. It has been demonstrated that electron shot noise provides a useful tool to detect the role played by electron coherence and Coulomb interactions and correlation in electronic transport through quantum dots^{15,22}. Besides

it provides information about current fluctuations that cannot be extracted from the average current alone^{20,21}.

There have been theoretical²³⁻²⁵ and experimental studies^{26,27} of the Kondo phenomena when the QD is connected to a quantum box, where the uncorrelated conducting electrons are described by a series of discrete energy levels. The finite system density of states consists of a series of peaks separated by an energy Δ inversely proportional to the number of sites N and, in a tight binding representation of the discrete system, proportionally to the hopping matrix elements v that connects the sites. The universal exponential dependence with the system parameters of the Kondo temperature is established in this case in the limit when the energy separation of the discrete levels of the quantum box is much less than the characteristic Kondo temperature that this system would have if the impurity were connected to a continuum conduction band. The behavior of a Kondo box, from the discrete to the continuum limit when the size of the box tends to infinite, has been studied^{23,28}. For the case of a QD connected to a quantum box able to be represented in the Fermi region by only one semi-occupied level, the energy of the singlet ground state is less than the energy of the excited triplet state by an amount that can be associated to a T_k of this discrete system. This T_k can be expanded in powers of the parameter $\gamma = t^2/\varepsilon_0$ where t is the non diagonal hopping matrix elements connecting the QD to the quantum box and ε_0 is the energy of the local QD level²⁹.

In the present work, we investigate the transport properties of a strongly correlated QD attached to two leads and to a quantum ring (QR) pierced by a magnetic flux, that in fact acts as a quantum box, which energies can be continuously modified by the application of the magnetic field. This system is conditioned by the interplay between two different Kondo effects, the bulk Kondo regime that

results from the connection of the QD to the leads and the Kondo box regime due to the interaction between the QD and the ring. Manipulating the parameters, the system presents unexplored very interesting crossover behavior. A schematic model of the structure proposed is shown in Fig. 1. We call the attention to the fact that this system possesses similarities to the one proposed to study the properties of a two channel Kondo system²⁶. However, the physics we are analyzing is completely different because our system does not have two independent channels as in this case the electrons can hop from the continuous to the discrete reservoir without any restrictions. There is no Coulomb correlation among the electrons within the QR to impede the free entrance of an electron when one of the discrete levels is in the nearby of the Fermi energy²⁶.

The crossover between the continuous Kondo and the Kondo box regimes can be studied by manipulating the connection of the QD to the leads and to the QR. The conductance, the current fluctuations and the Fano coefficient result to be the relevant physical magnitudes to be analyzed in the parameter space to reveal the physical properties of these two Kondo regimes and the crossover region between them. The physics of the QR acting as a quantum box and the crossover between the two regimes depend upon the spacing of the QR states in comparison with the Kondo temperature and on the quantum box being at resonance (off-resonance) when one of its states is (is not) at the neighborhood of the Fermi level. This last condition can be changed continuously by simply modifying the magnetic flux threading the ring.

The results are obtained using the SBMFT^{8,30,31} approach that is able to adequately describe the properties of the Kondo regime at very low energies, far apart from the mix-valence regime.

The paper is organized as follows. In Section II, we present the model, the Hamiltonian we used to study it, the central concepts regarding the SBMFA and the derivation of the analytical expression for the current I and shot noise S . In Section III, we briefly discuss the results for the LDOS and the transport properties corresponding to the different regimes of the system. Finally, we elaborate a summary of the paper in Section IV.

II. MODEL

We consider QD with e-e interaction, connected with two leads and with N sites QR. The Hamiltonian of the system outlined in Fig. 1 can be written as,

$$H = H_L + H_{QR} + H_{QD} + H_{L-QD} + H_{QD-QR}$$

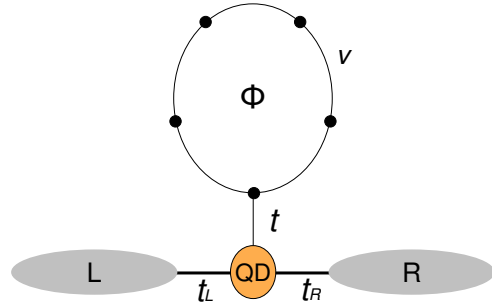


FIG. 1. Schematic diagram of quantum-dot attached to two leads and coupled to a quantum ring (quantum box) pierced by a magnetic flux.

where the different sub-Hamiltonian H_β are given by,

$$\begin{aligned} H_L &= \sum_{k_\alpha, \sigma, \alpha} \varepsilon_{k_\alpha} c_{k_\alpha, \sigma}^\dagger c_{k_\alpha, \sigma} + hc \\ H_{QR} &= \sum_{m, \sigma} \varepsilon_m(\Phi) a_{m, \sigma}^\dagger a_{m, \sigma} \\ H_{QD} &= \varepsilon_0(n_\uparrow + n_\downarrow) + U n_\uparrow n_\downarrow \\ H_{L-QD} &= \sum_{k_\alpha, \alpha} t_\alpha c_{k_\alpha, \sigma}^\dagger d_\sigma + hc \\ H_{QD-QR} &= \frac{t}{\sqrt{N}} \sum_{m, \sigma} a_{m, \sigma}^\dagger d_\sigma + hc \end{aligned} \quad (1)$$

where $\alpha = L, R, \varepsilon_m(\Phi) = -2v \cos(\frac{2\pi}{N}(\Phi/\Phi_0 + m))$ ($m = 1, \dots, m$) and $\Phi_0 = h/e$ is the quantum of flux. We consider the density of states describing the left (right) lead $\rho_{L(R)}$ as being constant and equal to $1/D$, where D is the lead bandwidth. The coupling strength between the QD and the leads is given by $\Gamma_{L(R)} = \pi \rho_{L(R)} t_{L(R)}^2$.

In the wide band limit ($D \gg 1$) and for infinite Coulomb repulsion ($U \rightarrow \infty$), $T_k = D e^{-\pi|\varepsilon_0|/\Gamma}$. It is necessary that $T < T_k$ for the system to have a Kondo behavior. When the temperature $T > T_k$, the spin correlations between the localized electron and the conduction electrons are eliminated by thermal fluctuation, driving the system out of Kondo regime. The Kondo ground state corresponds to a situation in which the QD is occupied by a one electron, which requires $\varepsilon_0 < -\Gamma$ and $(\varepsilon_0 + U) > \Gamma$. Otherwise, charge fluctuations are significant and the system is in a mixed valence regime.

The intra-dot Coulomb interaction U is not a relevant parameter for the Kondo effect if the QD is in the one electron Coulomb blockade regime. As a consequence, it is interesting to assume the $U \rightarrow \infty$ limit as it simplifies the self-consistent calculations because the QD in this case has only three available states: the empty state or the spin up or down electron occupied states³¹. It is convenient to rewrite the Hamiltonian H , projecting out the double QD occupancies. In order to do this, we use the slave boson approach³⁰. We define the operators f_σ^\dagger

(f_σ) that creates (destroys) the pseudo fermion of σ spin in the QD and b^\dagger (b) that creates (destroys) an empty pseudo bose state and impose a constraint that explicitly eliminates the double occupied state,

$$b^\dagger b + \sum_\sigma f_\sigma^\dagger f_\sigma = \mathbf{1}. \quad (2)$$

The use of an auxiliary field λ which acts as a Lagrange multiplier permits to impose the condition Eq.2. The Hamiltonian takes the form

$$\begin{aligned} H = & \sum_{k_\alpha\sigma,\alpha} \varepsilon_{k_\alpha} c_{k_\alpha\sigma}^\dagger c_{k_\alpha\sigma} + \sum_\sigma \varepsilon_0 f_\sigma^\dagger f_\sigma \\ & + \sum_m \varepsilon_m(\Phi) a_{m\sigma}^\dagger a_{m\sigma} + \frac{1}{\sqrt{2}} \sum_{k_\alpha\sigma,\alpha=L,R} t_\alpha c_{k_\alpha\sigma}^\dagger b^\dagger f_\sigma \\ & + \frac{t}{\sqrt{2N}} \sum_m a_{m\sigma}^\dagger b_\sigma^\dagger f_\sigma + \lambda (b^\dagger b + \sum_\sigma f_\sigma^\dagger f_\sigma - 1) \end{aligned} \quad (3)$$

Within the SBMFT approach³¹, we replace the bosonic operator by its expectation value $\langle b \rangle = \sqrt{2\tilde{b}}$ and assume that $\langle b^\dagger b \rangle \simeq \langle b \rangle^2 = 2\tilde{b}$. At temperature $T = 0$, SBMFT describes quite well the Kondo regime characterized by strong spin fluctuation, but it is not reliable in the charged fluctuating mixed valence region. This confines our analysis to $\varepsilon_0/(\Gamma_L + \Gamma_R) < -0.5$. Within this formalism, the Hamiltonian becomes a one-body effective one, \tilde{H} .

$$\begin{aligned} \tilde{H} = & \sum_{k\sigma\alpha} \varepsilon_{k_\alpha} c_{k_\alpha\sigma}^\dagger c_{k_\alpha\sigma} + \sum_\sigma \tilde{\varepsilon}_0 f_\sigma^\dagger f_\sigma + \sum_m \varepsilon_m(\Phi) a_{m\sigma}^\dagger a_{m\sigma} \\ & + \sum_{k_\alpha\sigma,\alpha} (\tilde{t}_\alpha c_{k_\alpha\sigma}^\dagger f_\sigma + h.c.) + \frac{\tilde{t}}{\sqrt{N}} \sum_{m,\sigma} (a_{m\sigma}^\dagger f_\sigma + h.c.) \\ & + \lambda(2\tilde{b}^2 - 1) \end{aligned} \quad (4)$$

where $\tilde{t}_{L(R)} = t_{L(R)}\tilde{b}$, $\tilde{t} = t\tilde{b}$ and $\tilde{\varepsilon}_0 = \varepsilon_0 + \lambda$ are renormalized parameters. By minimizing the expectation value of \tilde{H} , $\langle \tilde{H} \rangle$ with respect to \tilde{b} and λ , incorporating the constraint (Eq.2), we obtain,

$$\tilde{b}^2 = \frac{1}{2} - \frac{1}{2} \sum_\sigma \langle f_\sigma^\dagger f_\sigma \rangle. \quad (5)$$

We determine self-consistently the parameters \tilde{b} and λ in terms of the Fourier component of QDs lesser Green's function^{8,33} $G_{d,\sigma}^<(\omega) = i\langle f_\sigma^\dagger f_\sigma \rangle_\omega$,

$$\begin{aligned} \tilde{b}^2 = & \frac{1}{2} - \frac{i}{4\pi} \sum_\sigma \int_{-D}^D G_{d,\sigma}^<(\omega) d\omega \\ \lambda \tilde{b}^2 = & \frac{i}{4\pi} \sum_\sigma \int_{-D}^D (\omega - \tilde{\varepsilon}_{0\sigma}) G_{d,\sigma}^<(\omega) d\omega. \end{aligned} \quad (6)$$

The function $G_{d,\sigma}^<$ and the retarded Green's function $G_{d,\sigma}^r$ are obtained using Langreth analytic continuation

and Dyson equation respectively^{32,33}

$$\begin{aligned} G_{d,\sigma}^<(\omega) = & 2i \frac{f_L(\omega)\tilde{\Gamma}_L + f_R(\omega)\tilde{\Gamma}_R}{(\omega - \tilde{\varepsilon}_0 - \frac{Q(\omega)}{\sqrt{N}})^2 + (\tilde{\Gamma}_L + \tilde{\Gamma}_R)^2} \\ G_{d,\sigma}^r(\omega) = & \frac{1}{\omega - \tilde{\varepsilon}_0 - \frac{Q(\omega)}{\sqrt{N}} + i(\tilde{\Gamma}_L + \tilde{\Gamma}_R)} \end{aligned} \quad (7)$$

where $Q(\omega) = \sum_m \tilde{t}^2/(\omega - \varepsilon_m(\Phi))$ and $\tilde{\Gamma}_{L(R)} = \tilde{b}^2 \Gamma_{L(R)}$. In order to characterize the different regimes of the system and its transport properties, it is important to calculate the DOS at the QD. It is given by the expression,

$$\rho_{QD}(\omega) = -\frac{1}{\pi} \text{Im} G_{d,\sigma}^r(\omega). \quad (8)$$

On the other hand, the transmission probability $T(\omega, V)$ can be written,

$$T(\omega, V) = 4 \frac{\tilde{\Gamma}_L \tilde{\Gamma}_R}{\tilde{\Gamma}_L + \tilde{\Gamma}_R} \text{Im} [G_{d,\sigma}^r(\omega)]. \quad (9)$$

Note that the transmission depends on the applied bias V as it appears in the self-consistent equations Eq.6. The transport properties are studied at temperature $T = 0$. We calculate the current I transmitted through the QD, the shot noise S and the Fano factor $FF = S/2eI$. The current I and the shot noise S are given by,^{34,35}

$$\begin{aligned} I = & \frac{2e}{h} \int_{-eV/2}^{eV/2} T(\omega, V) d\omega, \\ S = & \frac{4e^2}{h} \int_{-eV/2}^{eV/2} T(\omega, V) [1 - T(\omega, V)] d\omega. \end{aligned} \quad (10)$$

III. NUMERICAL RESULT

In this section we discuss the transport properties at zero temperature $T = 0$. In what follows, we will consider $\Gamma_L = \Gamma_R = \Gamma$ as the energy unit and $E_F = 0$. We have taken the band-width to be $D = 35$ and set the QD energy level at $\varepsilon_0 = -3$. For these values $T_K = 1.4 \times 10^{-3}$ and $\sum_\sigma \langle f_\sigma^\dagger f_\sigma \rangle = 1 - T_K \approx 1$.

As already discussed in the introduction, in the Kondo box regime, the Kondo temperature of the equivalent continuous system is less than, or of the order of the energy separation of the quantum box states. In this regime, supposing an even number of electrons in the system, the energy difference between the ground singlet Kondo like state and the first excited triplet state is given by $4t^2/\varepsilon_0$ ²⁹, which permits this value to be associated to the Kondo temperature of the quantum box. As a consequence, to characterize the regime of the system it is convenient to compare this typical energy with

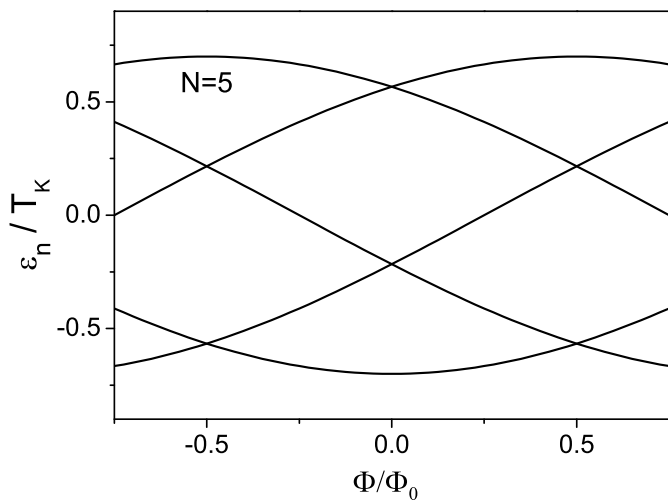


FIG. 2. Level spectrum of disconnected QR ($t = 0$), as a function of magnetic flux Φ for QR with $N = 5$ sites.

the Kondo temperature that results from the connection of the QD with the leads. This permits us to define a weak (strong) coupling regime when $t < \xi$ ($t > \xi$), with $\xi \equiv \sqrt{\varepsilon_0 T_K / 2}$.

As far as the quantum box is concerned the transport properties are affected by the QR energies $\varepsilon_n(\Phi)$ and its proximity to the Fermi level. The values of $\varepsilon_n(\Phi)$ are controlled by Φ , as shown in Fig. 2, while the spacing of the levels is dependent upon the magnitude v/N , being N the number of sites of the ring and v the hopping matrix element connecting them. As for numerical reasons it is better to take a small value of N , we arbitrarily assume $N = 5$ and a value of v , $v = 0.35T_k$, such that the few QR state energies are within the width of the Kondo peak of the QD attached to the leads and non connected to the ring. This is the condition for the properties of the Kondo regime, derived from the coexistence of a continuous and a discrete bath, to appear. Other possible states of a longer ring, far apart from the Fermi level, are not relevant for the physics we analyzed. We assume various magnetic fluxes Φ so as to manipulate the ring states relative to the Fermi level, studying in particular the situations when one state of the quantum ring is half occupied or the nearest states to the Fermi level are double or non-occupied.

In Fig.3 (a), (b), (c) and (d) we display the LDOS at the QD for weak, intermediate and strong coupling regimes respectively for $\Phi = 0$. In the weak coupling regime the LDOS is slightly perturbed by the ring states appearing as Fano anti-resonances in an otherwise clear Kondo peak that results from the QD connected to its left and right leads. This behavior can be understood by inspection of equation 7. The anti-resonances appear at the ring state energies, which are the poles of $Q(\omega)$. When the interaction with the ring increases the original Kondo peak is now highly perturbed and the DOS is now characterized by resonances that correspond to the poles of

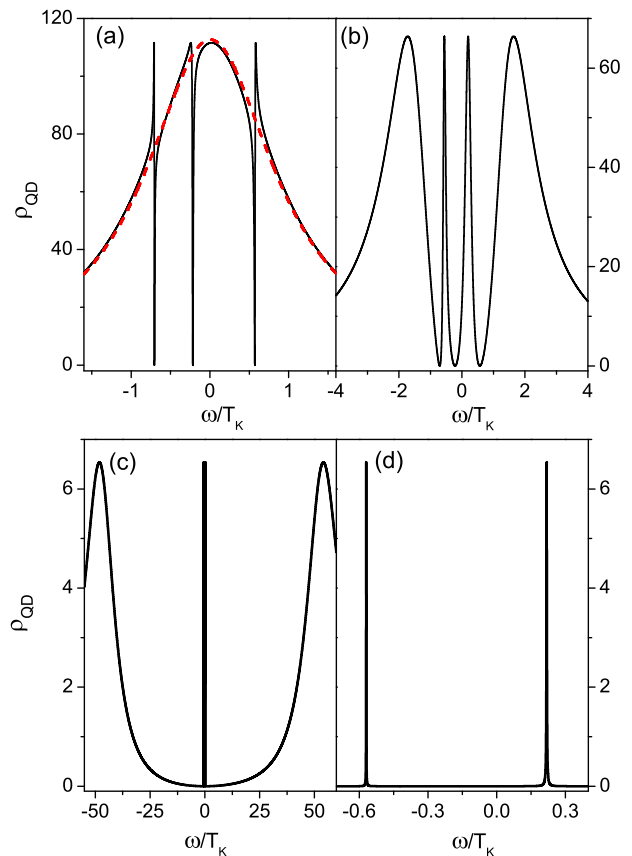


FIG. 3. (Color online) Density of states as a function of energy with magnetic flux $\Phi = 0$. In the panel (a) $t = 0.1\xi$ (solid black line) and for disconnected QR, $t = 0$ (red dashed line). In the panel (b) $t = \xi$ and in the panel (c) $t = 10\xi$. In the panel (d) it is shown in detail, the two central Lorentzian peaks for $t = 10\xi$.

the Green's function and by two side bands with energies that get more distant from the Fermi region as t increases. These side bands correspond originally to the continuum Kondo peak, splitted, is pushed away from the Fermi region. Well inside the strong regime in the Fermi region there are several discrete resonances of almost zero width while the continuum has been spread out from the Fermi region. This is clearly depicted in Fig.3(c) and (d). In this regime the impurity spin is completely screened by the spin of QR electrons near the Fermi level and there is no Kondo spin-spin correlation with the conducting electrons in the leads. It is very interesting to properly characterize these two regimes and the crossover between them. When the system is in the Kondo regime the renormalized local level of the QD, within the slave boson formalism, is fixed at the Fermi level independently of the gate potential applied to the QD, indicating the existence of a peak, the Abrikosov Shul resonance. This characteristic of the renormalized $\tilde{\varepsilon}_0$ is the finger print of the Kondo regime as far as the SBMFT formalism is concerned³⁶. In Fig. 5 we show the behavior of the $\tilde{\varepsilon}_0$ as a function of ε_0 . It is clear

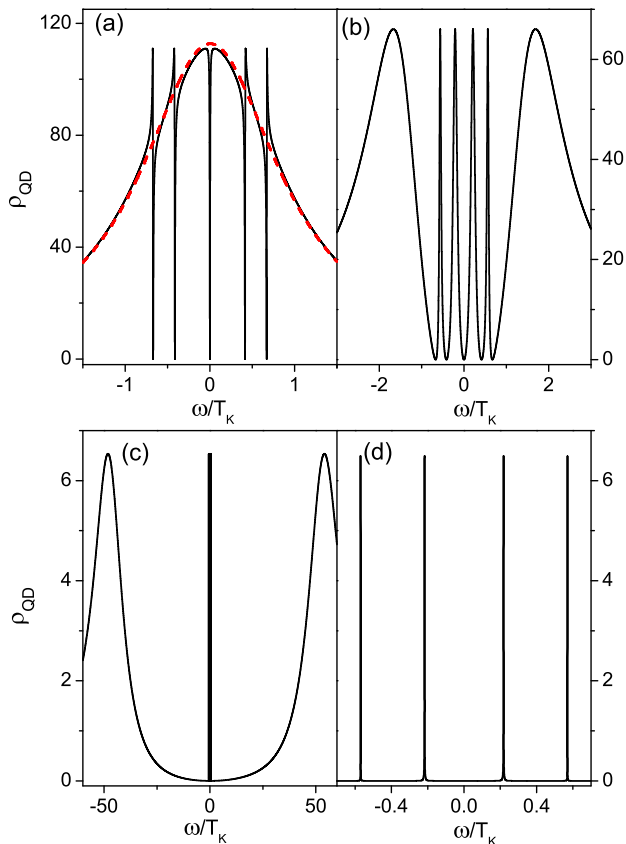


FIG. 4. (Color online) Density of states as a function of energy with magnetic flux $\Phi = 0.25\Phi_0$. In the panel (a) $t = 0.1\xi$ (black solid line) and for disconnected QR, $t = 0$ (red dashed line). In the panel (b) $t = \xi$ and in the panel (c) $t = 10\xi$. In the panel (d) it is shown in detail, the two central Lorentzian peaks for $t = 10\xi$

from the figure that independently of the system being in the weak or strong coupled regime the local level is renormalized to zero, when ε_0 is below the Fermi energy. In the weak coupled regime, as it is clearly shown by the continuous resonance at the Fermi level of the DOS, the system is in the traditional bulk Kondo regime. In the strong coupling regime, the Kondo peak appears as a bunch of discrete levels very concentrated at the Fermi level reflecting the fact that the system is in a Kondo like regime corresponding to an impurity connected to a quantum box, which has been named a Kondo box. As $\Phi = 0$ does not give rise to semi-occupied state of the QR because no ring state coincides with the Fermi energy, the screening of the QD spin by the QR spins is possible through virtual excitations of one electron of the nearest to the Fermi energy double occupied ring state to the nearest non-occupied one²³. This argument is not valid in presence of an external applied potential, if one of the level is tunned to be within the left and the right Fermi level in which case the state is semi-occupied and no virtual excitations are required to screened the QD spin.

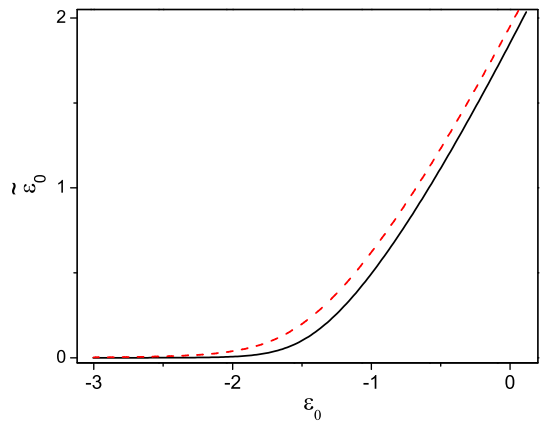


FIG. 5. (Color online) Renormalized energy vs gate voltage for weak coupling regime, $t = 0.4\xi$ (black solid line) and strong coupling regime, $t = 10\xi$ (red dashed line) for $\Phi = 0$.

We have a quantitative different situation when $\Phi = 0.25\Phi_0$ in which case the states in the ring are not degenerated and they are symmetrically distributed above and below the Fermi level with one of them, just at the Fermi level, occupied by only one electron as depicted in Fig. 2 and in the corresponding LDOS at the QD shown in Fig.4. In this case the emergence of the Kondo box regime is easier, it is reached for smaller values of t ²³. Within the scope of the SBMFT formalism this is the case because the renormalized energy $\tilde{\varepsilon}_0$ of the QD state interacts strongly with the QR state at the Fermi level, as both have the same energy, producing a bonding and anti-bonding state as can be seen in Fig.4(d). The anti-bonding state will be double occupied by two opposite spin electrons. This is the mechanism that can explain the anti-ferromagnetic correlation between the QD spin and the spin of the electron populating the state at the Fermi level of the QR, which gives rise to the Kondo box regime. However, as far as the essential physics we are analyzing is concerned, the behavior of the system in the strong coupling regime is only quantitatively weakly dependent on Φ , as can be concluded by inspection of Fig.3, 4.

In order to adequately characterize the different regimes of the system, we calculate the current I and the shot noise S as a function of the potential bias V for different coupling regimes. The Fig.6 displays I (S) in left (right) panels restricted to the $\Phi = 0$ case. In the weak and intermediate regime, the current and shot-noise increase smoothly with the potential bias. However, in the strong coupling regime S and I have steps for especial values of the external potential, which position depends upon ϕ . When the region between the left and right Fermi level includes a discrete local Kondo like peak, the current is able to flow increasing abruptly. Although this discrete states localized at the QD, as shown in Fig.3 and 4, are a resultant of the screening produced by the free spins in the QR, they provide a path for the electrons to go along, showing that these states have a su-

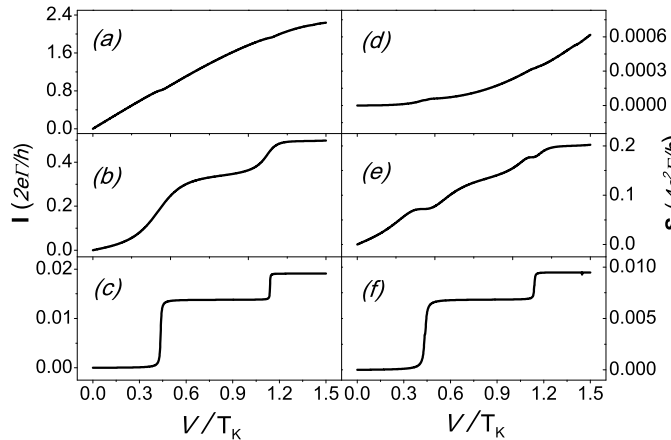


FIG. 6. Current (left panel) and Shot noise (right panel) versus bias voltage V , for magnetic flux $\Phi = 0$, and a) $t = 0.1\xi$, b) $t = \xi$ and c) $t = 10\xi$.

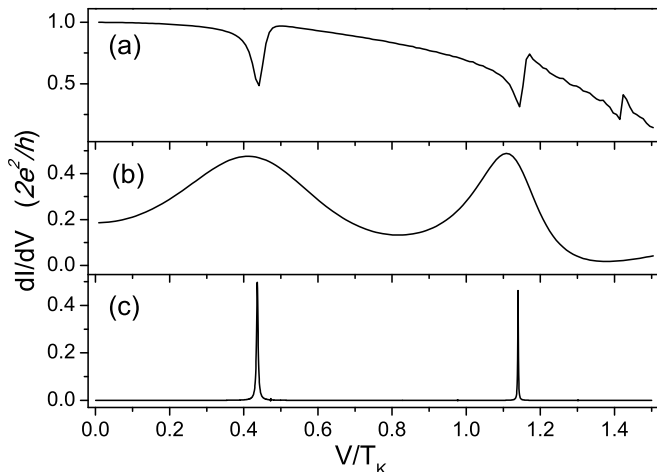


FIG. 7. Differential conductance as a function of applied voltage for $\Phi = 0$ and a) $t = 0.1\xi$, b) $t = \xi$ and c) $t = 10\xi$.

perposition with the leads. In the first plateau, the shot noise is $S = 2eI$ and in the last two $S = eI$ (Fig.6 (c) and (f)). The above results show that the measurement of the current and the noise permits to make a clear distinction and characterization of the regimes of the system. This is as well reflected in the differential conductance dI/dV , that is depicted in Fig.7 as a function of the bias. In the weak coupling regime, we can see that the differential conductance displays Fano anti-resonances any time that a level of the QR enter in the region between the left and the right Fermi energies. However in the strong coupling regime the differential conductance shows clear peaks corresponding to the steps in the current that were shown in Fig.6.

To complete the description of the transport properties, we study the Fano factor of the system. Fig. 8

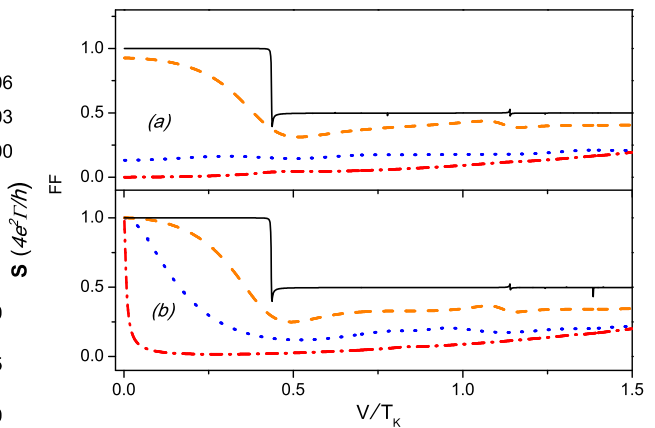


FIG. 8. (Color online). Fano factor versus bias, for two values of the magnetic flux, a) $\Phi = 0$ and b) $\Phi = 0.25\Phi_0$, for weak, intermediate and strong coupling regime, $t = 0.2\xi$ (red dashed-dotted line), $t = 0.6\xi$ (blue dotted line), $t = \xi$ (orange dashed line) and (solid black line) $t = 10\xi$

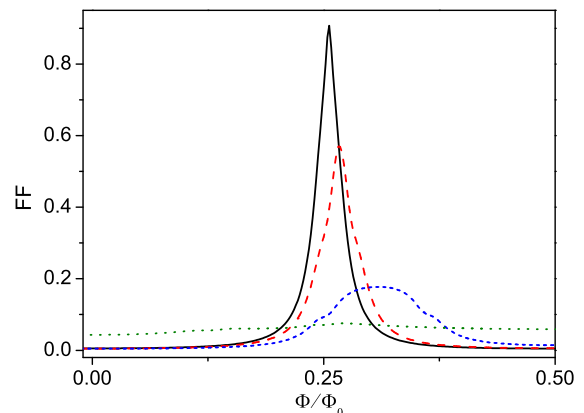


FIG. 9. (Color Online). Fano factor as function of the magnetic flux, for weak coupling regime ($t = 0.4\xi$) and different values of the bias. $V = 0.02T_k$ (black solid line), $V = 0.06T_k$ (red dashed line), $V = 0.2T_k$ (blue short dashed line), $V = T_k$ (green dotted line)

displays the Fano factor as a function of bias V , for two values of the magnetic flux, (a) $\Phi = 0$ and (b) $\Phi = 0.25$, for different QD-QR coupling in the range $0.4\xi < t < 10\xi$. In the strong coupling regime the Fano factor have two plateaus and drops from $FF = 1$ to $FF = 1/2$ at $V \approx 0.4T_k$. We observe this behavior for various values of the magnetic flux, showing that the Fano factor is independent on the flux in the Kondo box regime. On the other hand, in the weak coupling regime, $t = 0.1\xi$, the Fano factor profile depends strongly on the magnetic flux. As it is shown in Fig. 8 (a) for $\Phi = 0$ and $V \ll T_k$, the Fano-factor is $FF \ll 1$ and in Fig. 8 (b) for $\Phi = 0.25\Phi_0$, $FF \approx 1$.

In the strong coupling regime $S = 2eI$ in the first plateau, (see Fig.6) and hence $FF = 1$ and in the last two plateaus $S = eI$ or equivalently $FF = 1/2$.

This behavior is a consequence of the properties of the transmission probability $T(\omega, V)$ in the strong coupling regime. In the first plateau $T(\omega, V) \approx 0$, then,

$$[1 - T(\omega, V)] \times T(\omega, V) \approx T(\omega, V) \quad (11)$$

From Eqs.(10) and (11), it follows that in the first plateau $S = 2eI$. In the Kondo box regime, we can represent the transmission probability by a superposition of Briet-Wigner resonances.

$$T(\omega, V) = \sum_{\alpha} \frac{\tilde{\eta}^2}{(\omega - \tilde{\varepsilon}_{\alpha})^2 + \tilde{\eta}^2}, \quad (12)$$

where $\tilde{\varepsilon}_{\alpha}$ and $\tilde{\eta}$ are the positions and width of the Kondo box resonances, respectively. Then, from Eqs. 10 and 12 with $-V < \tilde{\varepsilon}_{\alpha} < V$, the current I and shot noise S can be written as follows,

$$I = \frac{4e}{h} M \tilde{\eta} \arctan\left(\frac{V}{\tilde{\eta}}\right)$$

$$S = \frac{4e^2}{h} M \tilde{\eta} \frac{[(\frac{V}{\tilde{\eta}})^2 + 1] \arctan(\frac{V}{\tilde{\eta}}) - \frac{V}{\tilde{\eta}}}{(\frac{V}{\tilde{\eta}})^2 + 1}. \quad (13)$$

where M is the number of resonances in the range of the applied bias. In the limit $V/\tilde{\eta} \gg 1$, $I \simeq 2\pi e \tilde{\eta}/h$ and $S \simeq 2\pi e^2 \tilde{\eta}/h$ or equivalently $S = eI$ and $FF = 1/2$, in agreement with the numerical results.

Finally, we calculate the Fano factor as a function of the magnetic flux for different values of the bias, in the weak coupling regime ($t = 0.4\xi$). As already discussed, the strong coupling regime is almost independent of Φ . The results are depicted in Fig.9. For small bias $V \ll T_k$, the Fano factor has a strong dependence on the magnetic flux, with a maximum around $\Phi = 0.25\Phi_0$. When the magnetic flux is $\Phi \approx 0.25\Phi_0$ the side coupled QR, as it can be observed in Fig.2, provides an state of energy $\varepsilon_n(0.25\Phi_0) = E_F = 0$ that can be visited by an electron which interferes destructively with the electron that goes directly through the QD. As a consequence the current intensity decrease and the Fano factor reaches it's maximal allowed value, $FF = 1$. Away of the maximum, all QR energy levels are far enough from the Fermi energy and the direct transport through QD predominates without any destructive interference. Then the ratio $S/2eI \ll 1$ and $FF \approx 0$. By increasing the bias up $V = T_k$, the Fano factor becomes almost independent of the magnetic flux. As the Fano factor is almost independent of the magnetic flux in the strong coupling Kondo box regime, as discussed above, the experimental measurement of this factor is another clear way of characterizing the system

We demonstrate that the differential conductance, the shot noise and the Fano coefficients are all measurable properties that allow a very detailed characterization of the two Kondo regimes and the crossover region that the system goes through by manipulating its parameters.

IV. SUMMARY

In this work, we investigate the properties of a very interesting Kondo phenomena that results from the interplay between the traditional bulk Kondo effect and the so-called Kondo box regime. We study the transport properties of a strongly correlated quantum dot attached to two leads and to a quantum ring (QR) pierced by a magnetic flux. In this system the QR acts as a quantum box, which energies can be continuously modified by the application of the magnetic field. The crossover between these two regimes was studied by changing the connection of the QD to the leads and to the QR.

In the weak coupling regime, we have showed that the differential conductance develops a sequence of Fano-Kondo antiresonances as a consequence of destructive interferences between the N discrete quantum ring levels with the conducting Kondo channel provided by the leads. In the strong coupling regime the differential conductance has very sharp resonances when one of the Kondo discrete sub-level characterizing the Kondo box is tuned by the applied potential. We were able to demonstrate that the conductance, the current fluctuations and the Fano factor result to be the relevant physical magnitudes to be analyzed in the parameter space to reveal the physical properties of these two Kondo regimes and the crossover region between them.

The transport properties of this system are so extremely dependent upon it parameters that it could have interesting potential applications as an active part of a nanoscopic circuit.

ACKNOWLEDGMENTS

V.M.A and P.A.O acknowledges support from CONICYT PSD 65. M.P and P.A.O acknowledges support from FONDECYT program Grants No. 1100560, and No. 1100672 and E.V. A. acknowledges support from the brazilian financial agencies FAPERJ(CNS program) and CNPq (BP and CIAM).

¹ L.I.Glazman, M.É. Raikh, JETP Lett. **47**, 452 (1988); Tai Kai Ng and Patrick A. Lee, Phys. Rev. Lett. **61**, 1768 (1988);

² D. Goldhaber-Gordon, H. Shtrikman, D. Mahalu, D. Abusch-Magder, U. Meirav, M. A. Kastner, Nature **391**, 156 (1998); D. Goldhaber-Gordon, J. Göres, M. A. Kast-

- ner, H. Shtrikman, D. Mahalu, U. Meirav, Phys. Rev. Lett. **81**, 5225 (1998).
- ³ S. M. Cronenwett, T. H. Oosterkamp, L. P. Kouwenhoven, Science **281**, 540 (1998).
 - ⁴ J. Göres, D. Goldhaber-Gordon, S. Heemeyer, M. A. Kastner, H. Shtrikman, D. Mahalu, U. Meirav, Phys. Rev. B **62**, 2188 (2000).
 - ⁵ U. Fano, Phys. Rev. **124**, 1866 (1961).
 - ⁶ Kensuke Kobayashi, Hisashi Aikawa, Shingo Katsumoto, and Yasuhiro Iye Phys. Rev. Lett. **88**, 256806 (2002).
 - ⁷ Masahiro Sato, Hisashi Aikawa, Kensuke Kobayashi, Shingo Katsumoto, and Yasuhiro Iye Phys. Rev. Lett. **95**, 066801 (2005).
 - ⁸ B. H. Wu, J. C. Cao, and K. H. Ahn, Phys. Rev. B **72**, 165313 (2005).
 - ⁹ J. Kondo, Prog. Theor. Phys. **32**, 37 (1964).
 - ¹⁰ P. A. Orellana, G. A. Lara and E. V. Anda, Phys. Rev. B **74**, 193315 (2006).
 - ¹¹ P. A. Orellana, M. L. Ladrón de Guevara, and F. Claro, Phys. Rev. B **70**, 233315 (2004).
 - ¹² M.A. Davidovich, E. V. Anda, C.A. Busser and G. Chiappe, Phys. Rev. B **65**, 233310 (2002)
 - ¹³ Piotr Trocha, Josef Barnas, Phys. Rev. B **78** 075424 (2008).
 - ¹⁴ Ya M Blanter and M. Büttiker, Phys. Rep. **336**, 1 (2000).
 - ¹⁵ Bing Dong and X. L. Lei J.Phys: Condens. Matt. **14**, 4963 (2002).
 - ¹⁶ M. Reznikov, M. Heiblum, H. Shtrikman, D. Mahalu, Phys. Rev. Lett. **75**, 3340 (1995).
 - ¹⁷ Shuji Nakamura, Masayuki Hashisaka, Yoshiaki Yamauchi, Shinya Kasai, Teruo Ono, and Kensuke Kobayashi, Phys. Rev. B **79**, 201308(R) (2009).
 - ¹⁸ Shuji Nakamura, Yoshiaki Yamauchi, Masayuki Hashisaka, Kensaku Chida, Kensuke Kobayashi, Teruo Ono, Renaud Leturcq, Klaus Ensslin, Keiji Saito, Yasuhiro Utsumi, and Arthur C. Gossard Phys. Rev. Lett. **104**, 080602 (2010).
 - ¹⁹ Masayuki Hashisaka, Yoshiaki Yamauchi, Shuji Nakamura, Shinya Kasai, Teruo Ono, and Kensuke Kobayashi, Phys. Rev. B **78**, 241303(R) (2008)
 - ²⁰ Reinhold Egger, Nature Physics **5**, 175 (2009).
 - ²¹ T. Delattre, C. Feuillet-Palma, L. G. Herrmann, P. Morfin, J.-M. Berroir, G. Fève, B. Plaçais, D. C. Glattli, M.-S. Choi, C. Mora, and T. Kontos, Nature Physics **5**, 208 (2009).
 - ²² Levy A.Yeyati, F. Flores, E.V. Anda, Phys. Rev B **47**, 10543 (1993)
 - ²³ Wolfgang B. Thimm, Johann Kroha and Jan von Delft, Phys. Rev. Lett. **82**, 2143 (1999)
 - ²⁴ Rainer Bedrich, Sebastien Burdin, and Martina Hentschel, Phys. Rev. B **81**, 174406 (2010).
 - ²⁵ Pascal Simon, Julien Salomez, and Denis Feinberg, Phys. Rev. B **73**, 205325 (2006).
 - ²⁶ R. M. Potok, I. G. Rau, Hadas Shtrikman, Yuval Oreg and D. Goldhaber-Gordon, Nature **446**, 167 (2007).
 - ²⁷ S. Sasaki, H. Tamura, T. Akazaki, and T. Fujisawa, Phys. Rev. Lett. **103**, 266806 (2009).
 - ²⁸ P. Simon and I. Affleck, Phys. Rev. Lett. **89**, 206602 (2002). Phys. Rev. B **68**, 115304 (2003).
 - ²⁹ Peter Fulde, Electron Correlations in Molecules and Solids, Springer-Verlag
 - ³⁰ P. Coleman, Phys. Rev. B **29**, 3035 (1984).
 - ³¹ D.M: News and N. Read, Adv. in Phys. **36**, 799 (1987).
 - ³² H.Haug and A. P. Jauho, Quantum Kinetics in Transport and Optics of Semiconductors (Springer-Verlag, Berlin), 1998.
 - ³³ D. C. Langreth, In Linear and Nonlinear Electron Transport in Solids (Plenum, New York), (1976).
 - ³⁴ Y. Meir and N. S. Wingreen, Phys. Rev. Lett. **68**, 2512 (1992).
 - ³⁵ R. Lopez, R. Aguado, and G. Platero, Phys. Rev. B **69**, 235305 (2004).
 - ³⁶ L. C. Ribeiro, E. Vernek, G. B. Martins, and E. V. Anda, Phys. Rev. B **85**, 165401 (2012).